

Catechol-based macrocyclic aromatic ether-sulfones: Synthesis, characterization and ring-opening polymerization

Article

Supplemental Material

Creative Commons: Attribution 4.0 (CC-BY)

Open Access

Aricò, F. and Colquhoun, H. M. (2021) Catechol-based macrocyclic aromatic ether-sulfones: Synthesis, characterization and ring-opening polymerization. ARKIVOC, 2021 (6). pp. 13-25. ISSN 1551-7004 doi: <https://doi.org/10.24820/ark.5550190.p011.424> Available at <https://centaur.reading.ac.uk/95231/>

It is advisable to refer to the publisher's version if you intend to cite from the work. See [Guidance on citing](#).

Identification Number/DOI: <https://doi.org/10.24820/ark.5550190.p011.424>
[<https://doi.org/10.24820/ark.5550190.p011.424>](https://doi.org/10.24820/ark.5550190.p011.424)

Publisher: Arkat USA

All outputs in CentAUR are protected by Intellectual Property Rights law, including copyright law. Copyright and IPR is retained by the creators or other copyright holders. Terms and conditions for use of this material are defined in the [End User Agreement](#).

www.reading.ac.uk/centaur

CentAUR

Central Archive at the University of Reading
Reading's research outputs online

Supplementary Material

Catechol-based macrocyclic aromatic ether-sulfones: Synthesis, characterization and ring-opening polymerization

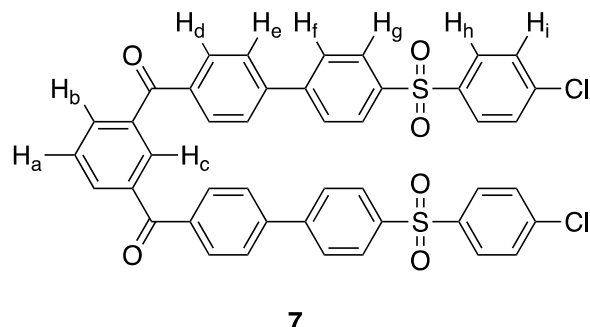
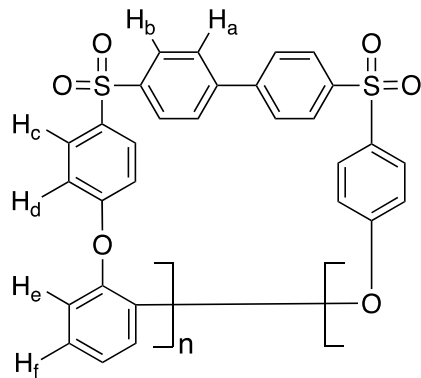
Fabio Aricò^{*a} and Howard M. Colquhoun^{*b}

^a*Department of Environmental Sciences, Informatics and Statistics, Ca' Foscari University,
Via Torino 155, 30172 Venice, Italy*

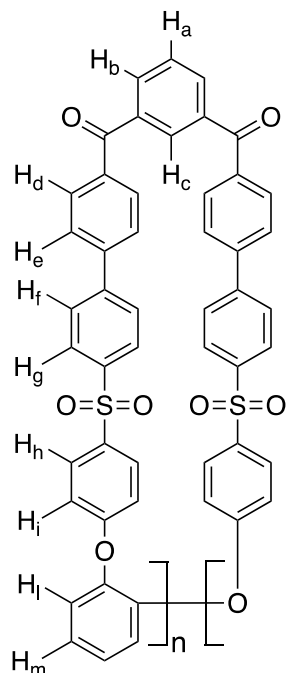
^b*Department of Chemistry, University of Reading, Whiteknights, Reading, RG6 6AD, UK
Email: fabio.arico@unive.it; h.m.colquhoun@rdg.ac.uk*

Table of Contents

Chart S1: Labelled structures for ^1H NMR assignments.....	S2
Figure S1: ^1H NMR spectrum of macrocycle 2	S3
Figure S2: ^{13}C NMR spectrum of macrocycle 2	S3
Figure S3: MALDI-TOF mass spectrum of macrocycle 2	S4
Figure S4: ^1H NMR spectrum of macrocycle 3	S5
Figure S5: ^{13}C NMR spectrum of macrocycle 3	S5
Figure S6: MALDI-TOF mass spectrum of macrocycle 3	S6
Figure S7: ^1H NMR spectrum of macrocycle 4	S7
Figure S8: ^{13}C NMR spectrum of macrocycle 4	S7
Figure S9: MALDI-TOF mass spectrum of macrocycle 4	S8
Figure S10: ^1H NMR spectrum of macrocycle 5	S9
Figure S11: ^{13}C NMR spectrum of macrocycle 5	S9
Figure S12: MALDI-TOF mass spectrum of macrocycle 5	S10
Figure S13: ^1H NMR spectrum of linear oligomer 7	S11
Figure S14: ^{13}C NMR spectrum of linear oligomer 7	S11
Figure S15: MALDI-TOF mass spectrum of linear oligomer 7	S12
Figure S16: ^1H NMR spectrum of macrocycle 8	S13
Figure S17: ^{13}C NMR spectrum of macrocycle 8	S13
Figure S18: ^1H - ^1H COSY NMR spectrum of macrocycle 8	S14
Figure S19: MALDI-TOF mass spectrum of macrocycle 8	S15
Figure S20: ^1H NMR spectrum of macrocycle 9	S16
Figure S21: ^{13}C NMR spectrum of macrocycle 9	S16
Figure S22: MALDI-TOF mass spectrum of macrocycle 9	S17
Computational modelling of macrocycles 8 and 9	S17



2 ($n = 2$), **3** ($n = 3$), **4** ($n = 4$), **5** ($n = 5$)



8 ($n = 1$), **9** ($n = 2$)

Chart S1: Labelled structures for ^1H NMR assignments (refer to Experimental Section).

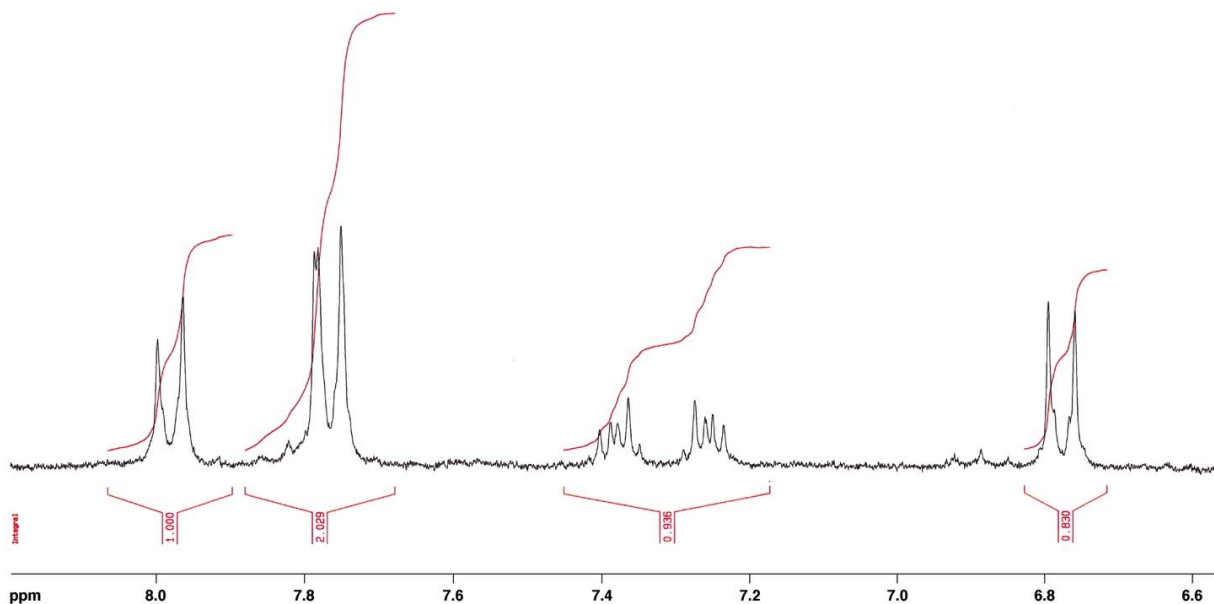


Figure S1: ¹H NMR spectrum of macrocycle 2 (250 MHz, CD₂Cl₂/CH₃SO₃H 4/1 v/v).

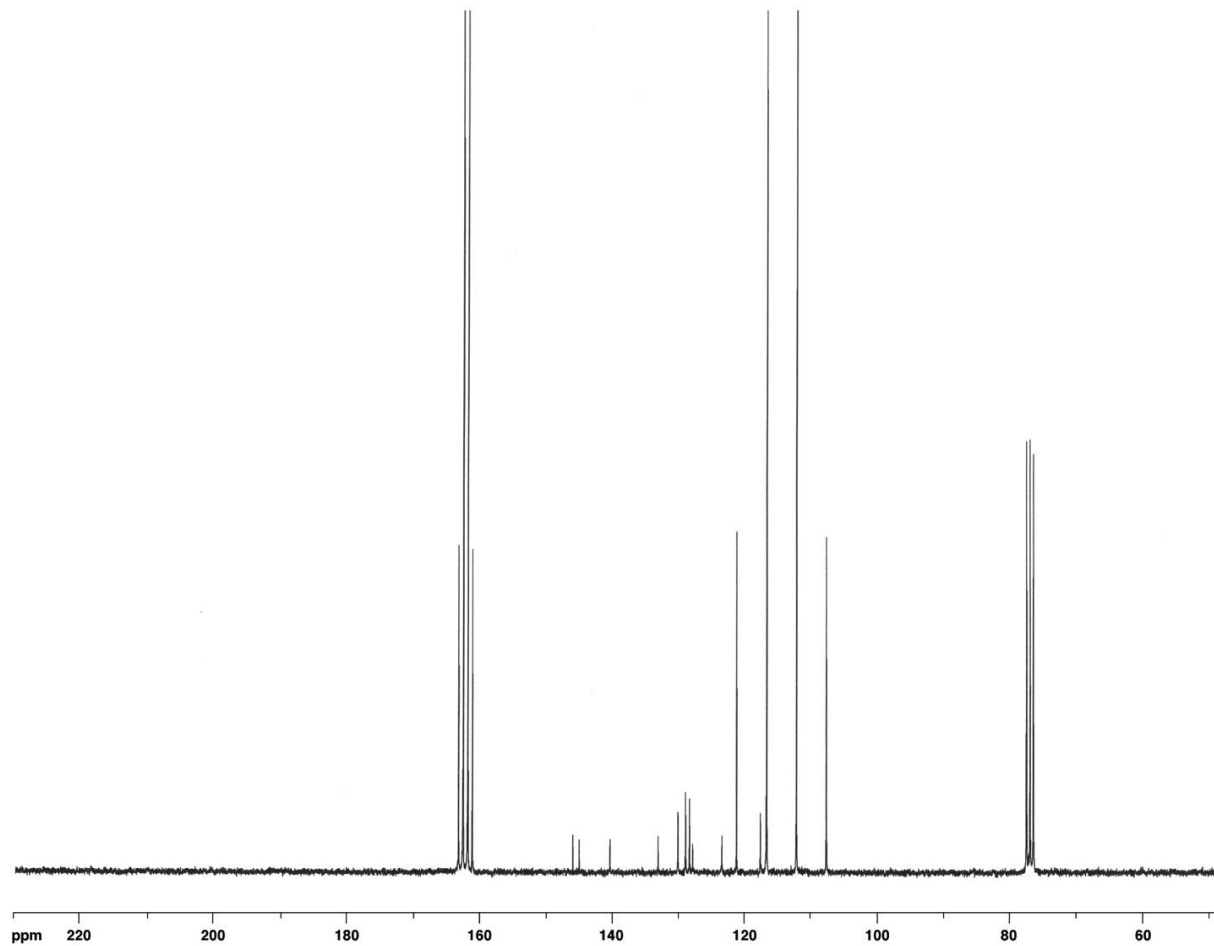


Figure S2: ¹³C NMR spectrum of macrocycle 2 (62.5 MHz, CDCl₃/CF₃CO₂H 5/1 v/v). Note: the strong quartet resonances centred at 114 and 162 ppm are due to trifluoroacetic acid co-solvent.

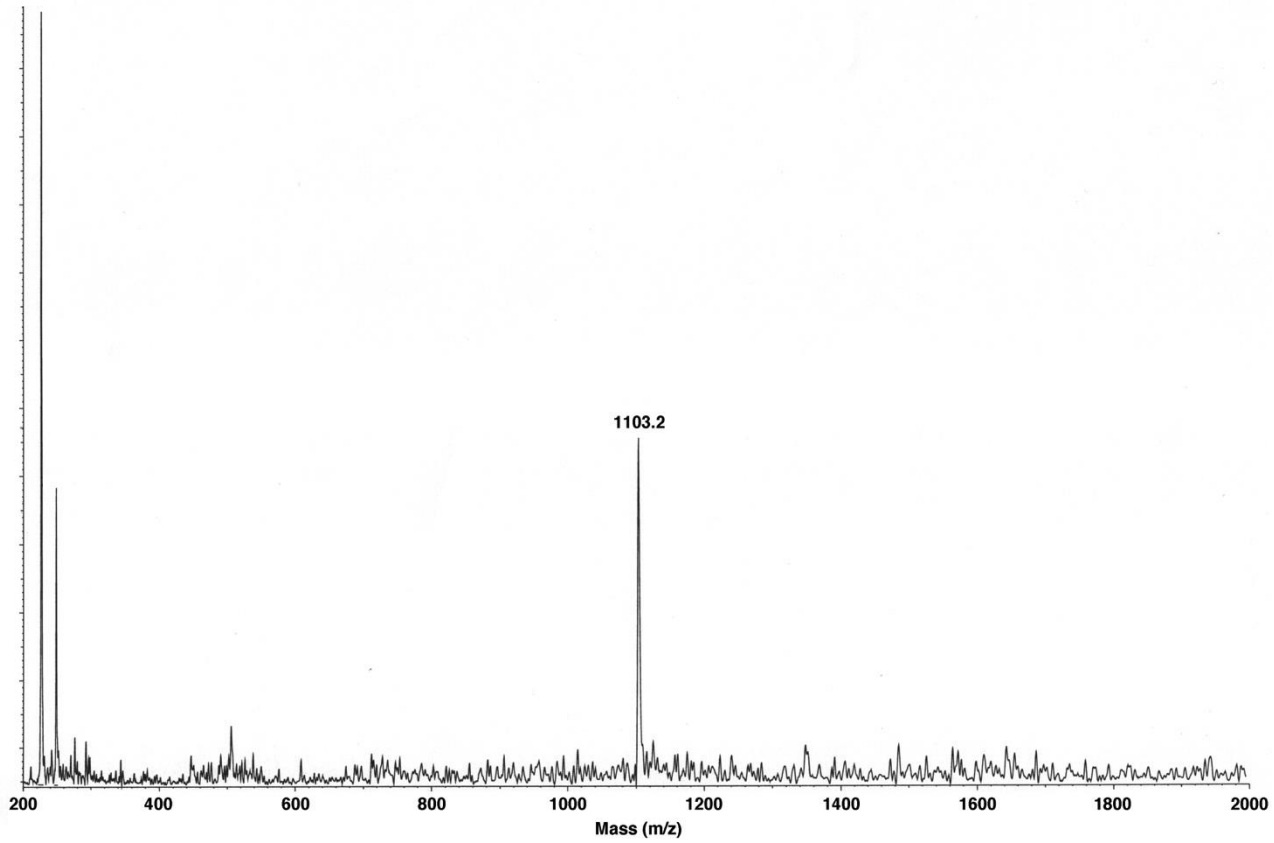


Figure S3: MALDI-TOF mass spectrum of macrocycle **2**. (Calc. m/z for $[C_{60}H_{40}S_4O_{12}Na]^+ = 1104.2$).

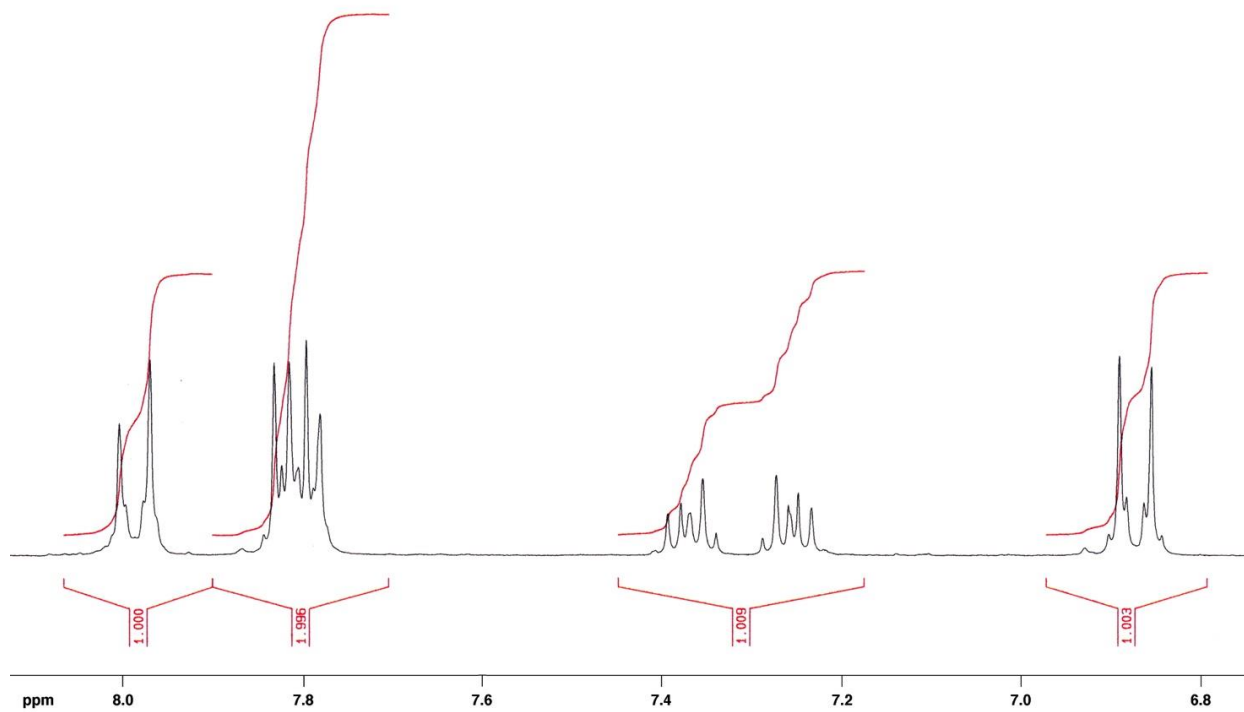


Figure S4: ¹H NMR spectrum of macrocycle 3 (250 MHz, CD₂Cl₂/CH₃SO₃H 4/1 v/v).

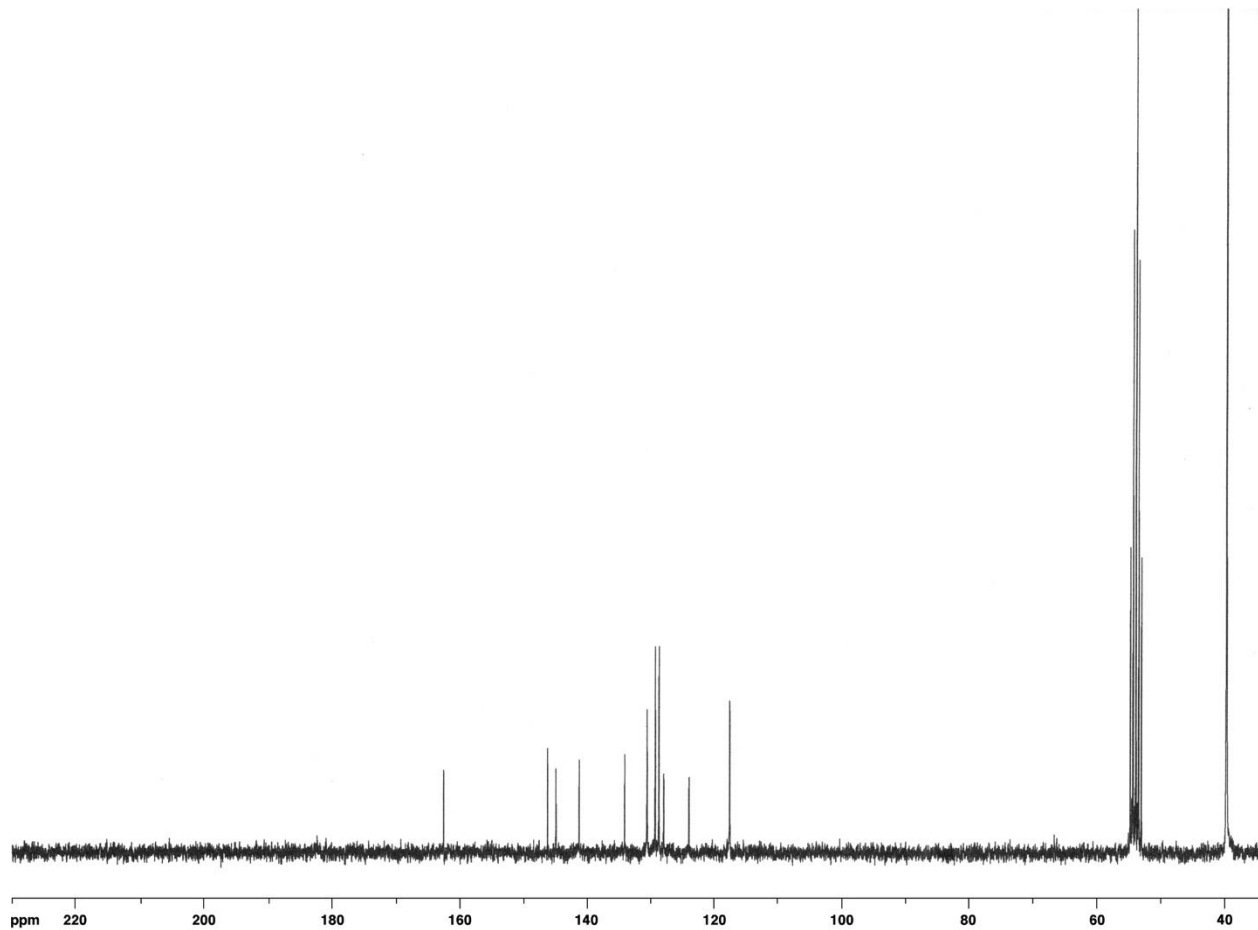


Figure S5: ¹³C NMR spectrum of macrocycle 3 (62.5 MHz, CD₂Cl₂/CH₃SO₃H 4/1 v/v).

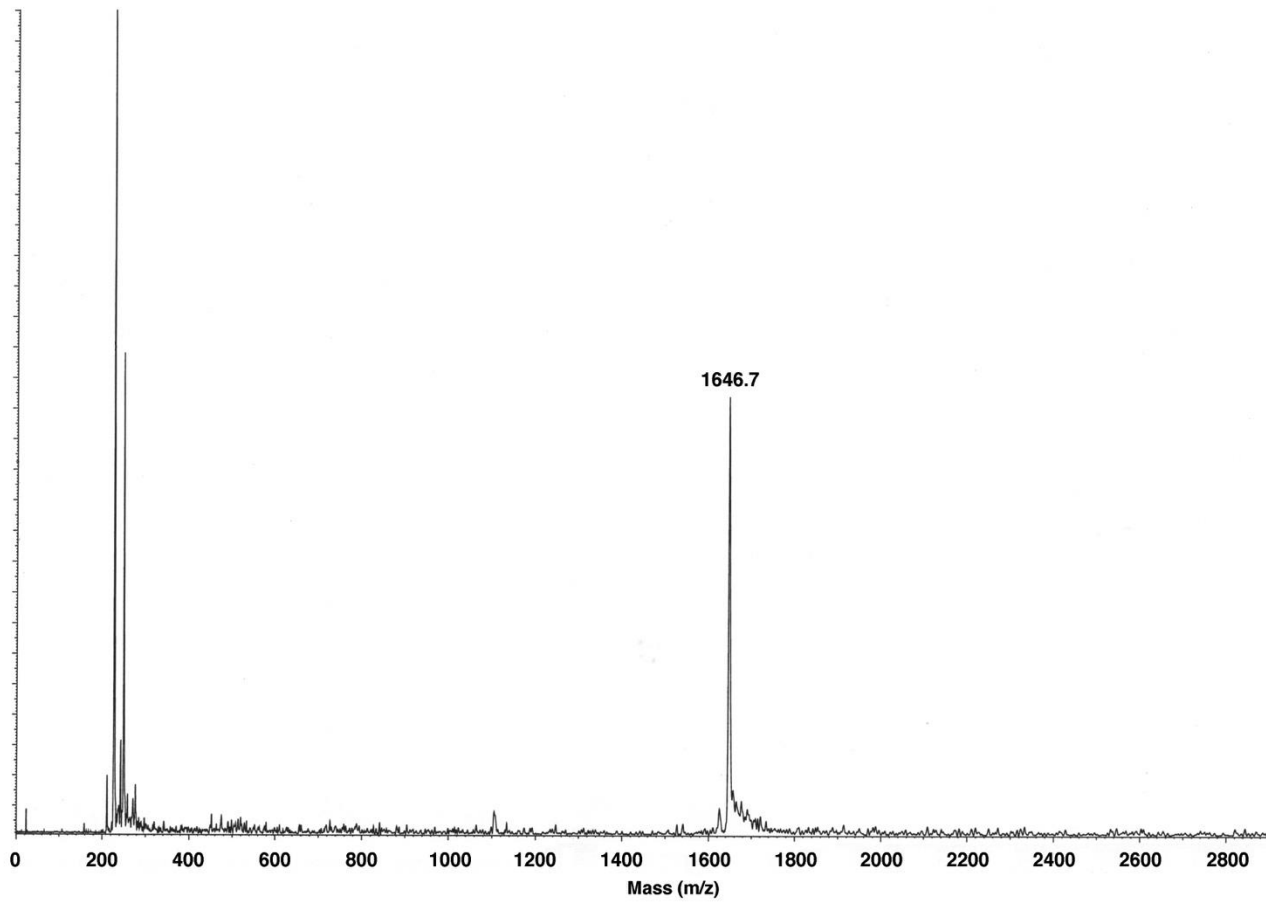


Figure S6: MALDI-TOF mass spectrum of macrocycle **3**. (Calc. m/z for $[C_{90}H_{60}S_6O_{18}Na]^+ = 1644.8$).

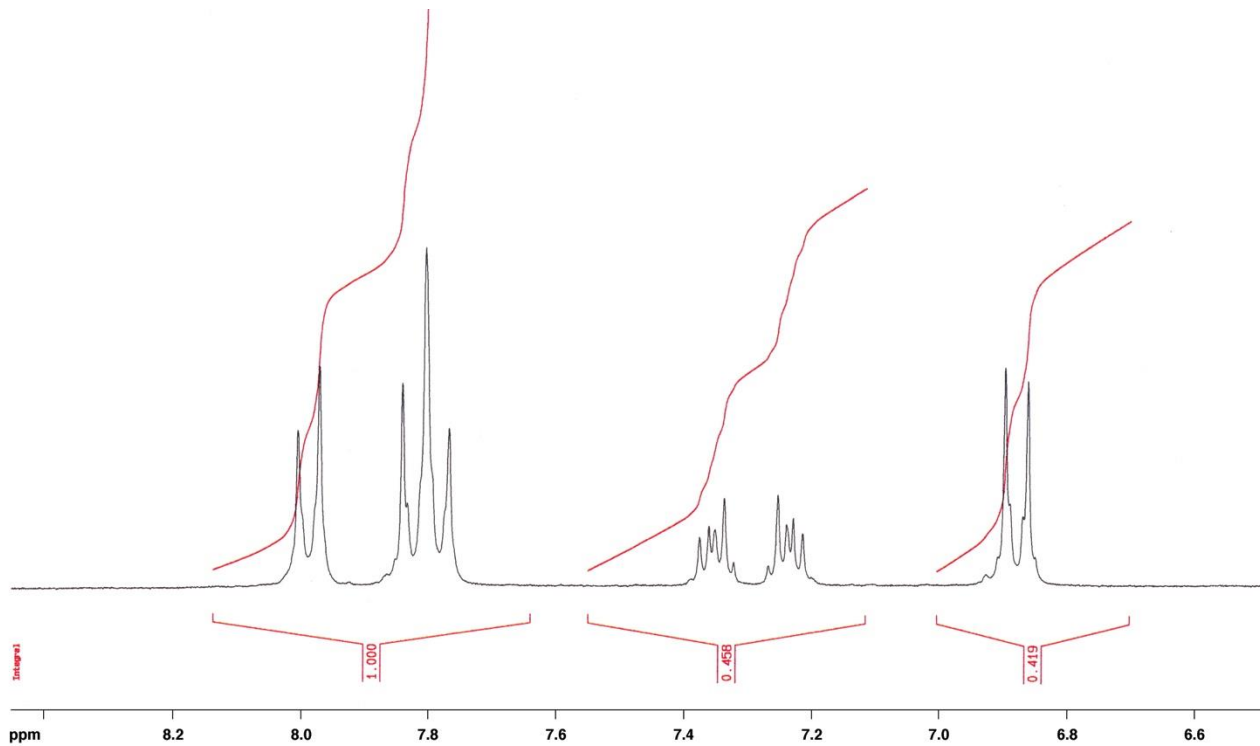


Figure S7: ¹H NMR spectrum of macrocycle 4 (250 MHz, CD₂Cl₂/CH₃SO₃H 4/1 v/v).

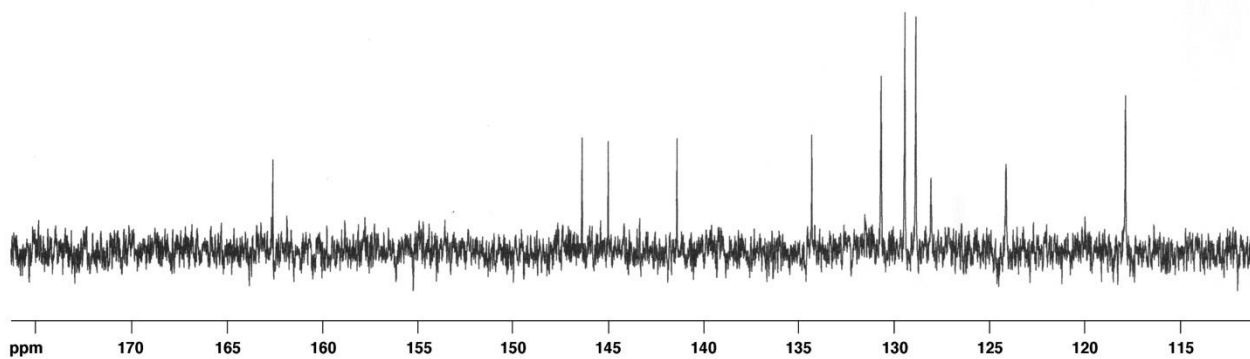


Figure S8: ¹³C NMR spectrum of macrocycle 4 (62.5 MHz, CD₂Cl₂/CH₃SO₃H 4/1 v/v).

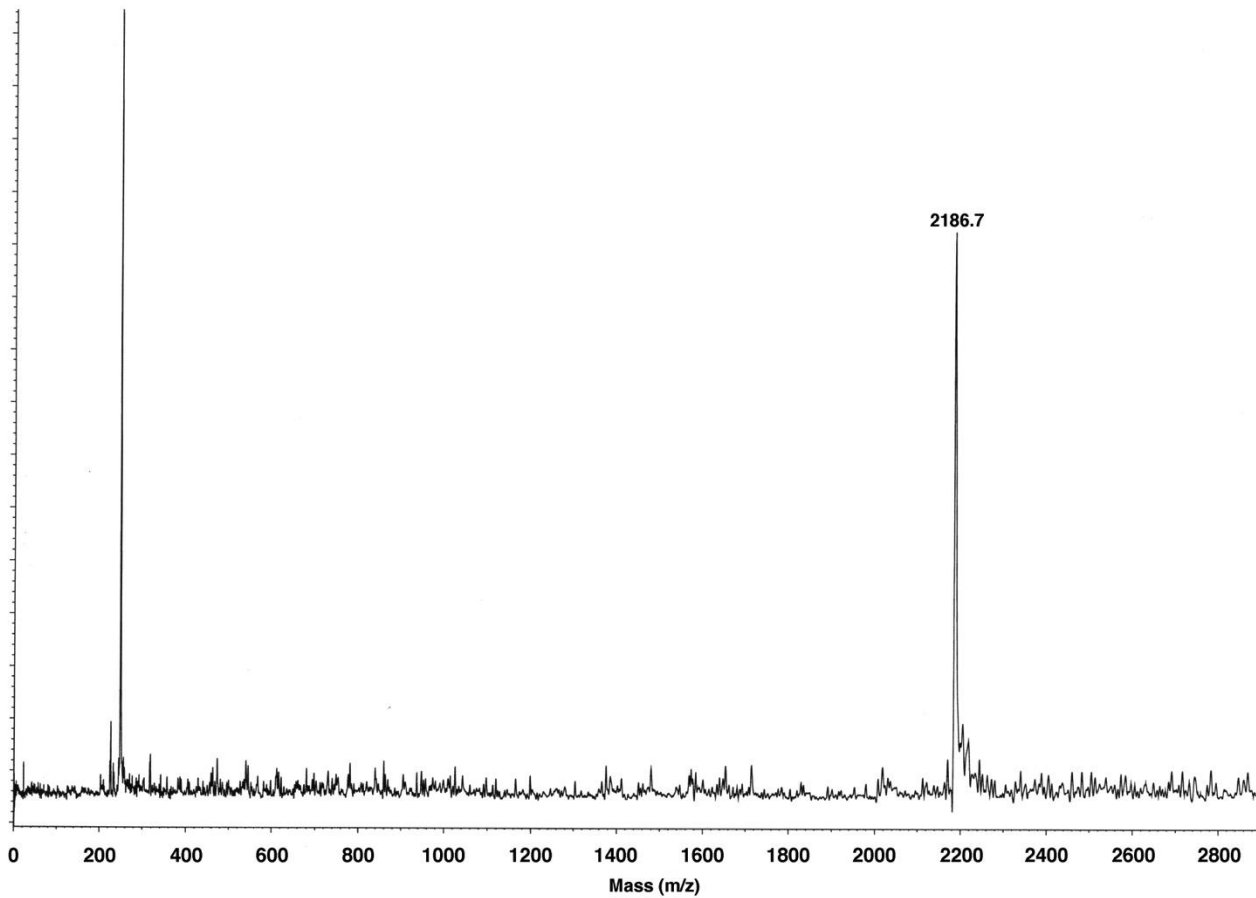


Figure S9: MALDI-TOF mass spectrum of macrocycle **4**. (Calc. m/z for $[C_{120}H_{80}S_8O_{24}Na]^+ = 2185.4$).

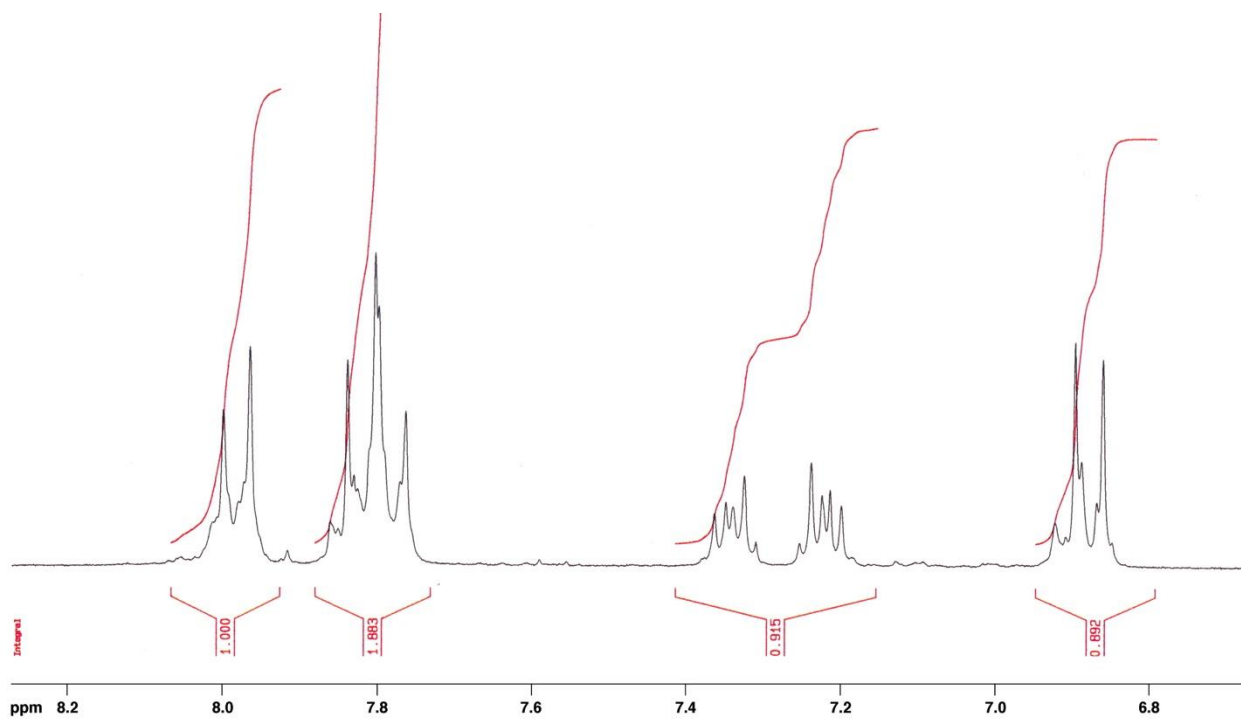


Figure S10: ¹H NMR spectrum of macrocycle 5 (250 MHz, CD₂Cl₂/CH₃SO₃H 4/1 v/v).

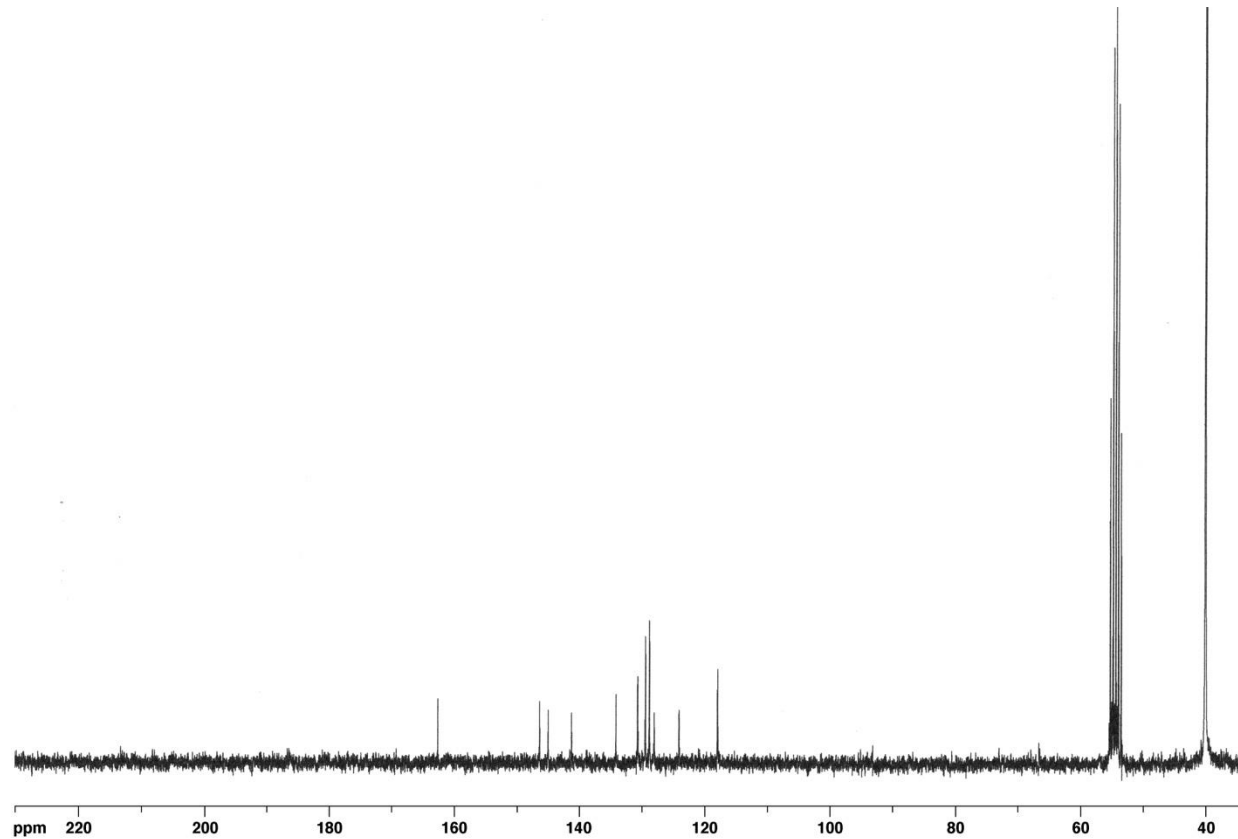


Figure S11: ¹³C NMR spectrum of macrocycle 5 (62.5 MHz, CD₂Cl₂/CH₃SO₃H 4/1 v/v).

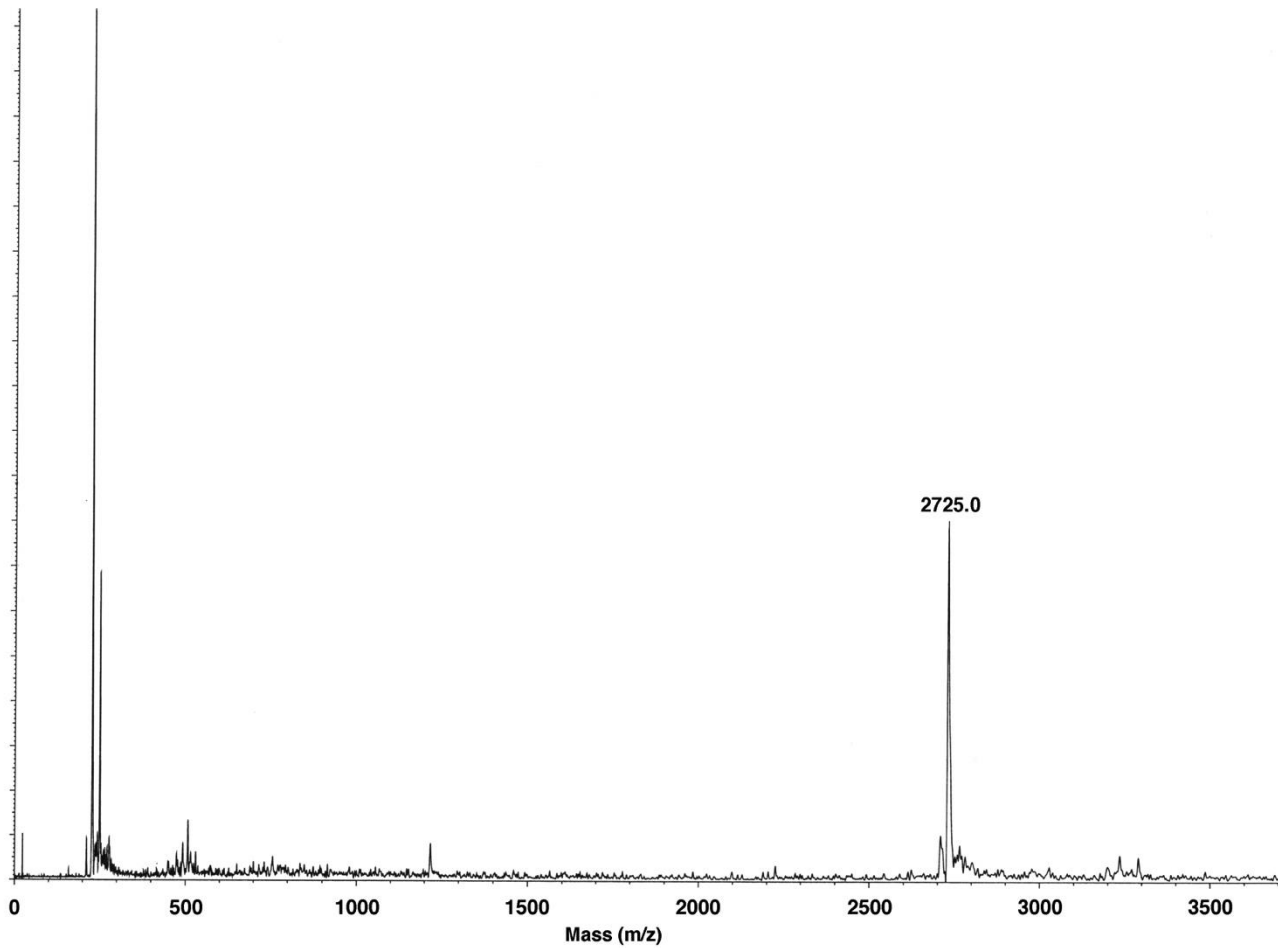


Figure S12: MALDI-TOF mass spectrum of macrocycle 5. (Calc. m/z for $[C_{150}H_{100}S_{10}O_{30}Na]^+$ = 2726.0).

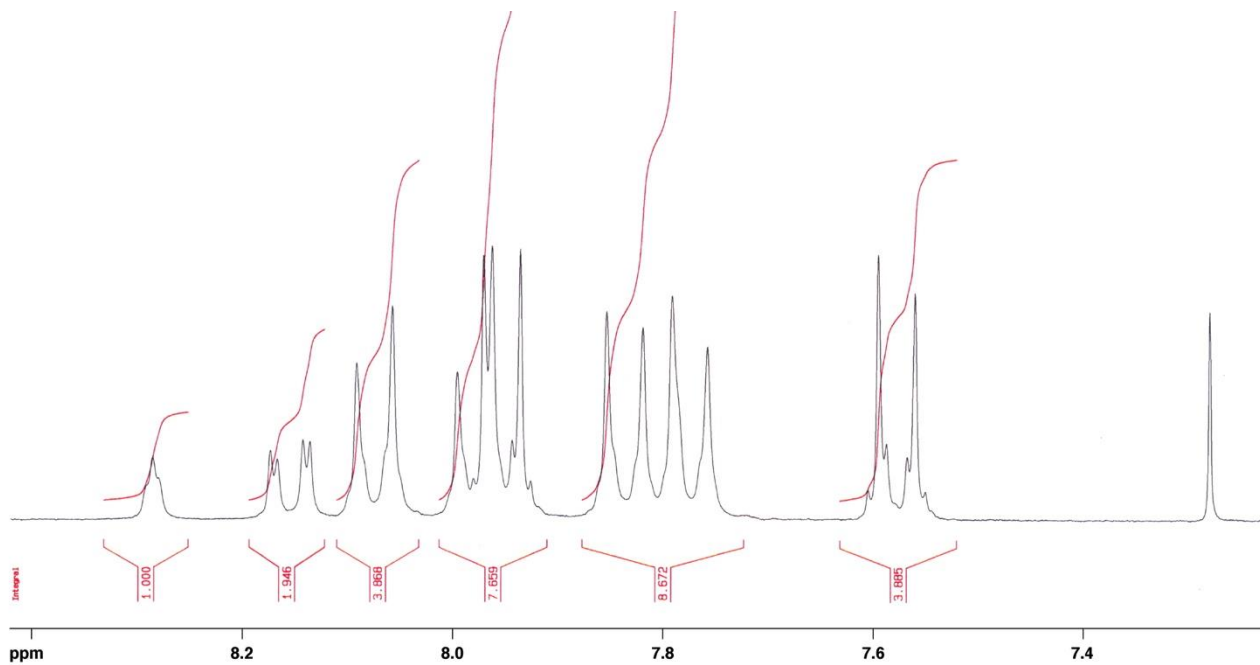


Figure S13: ¹H NMR spectrum of linear oligomer 7 (250 MHz, CDCl₃/CF₃COOH 5/1 v/v).

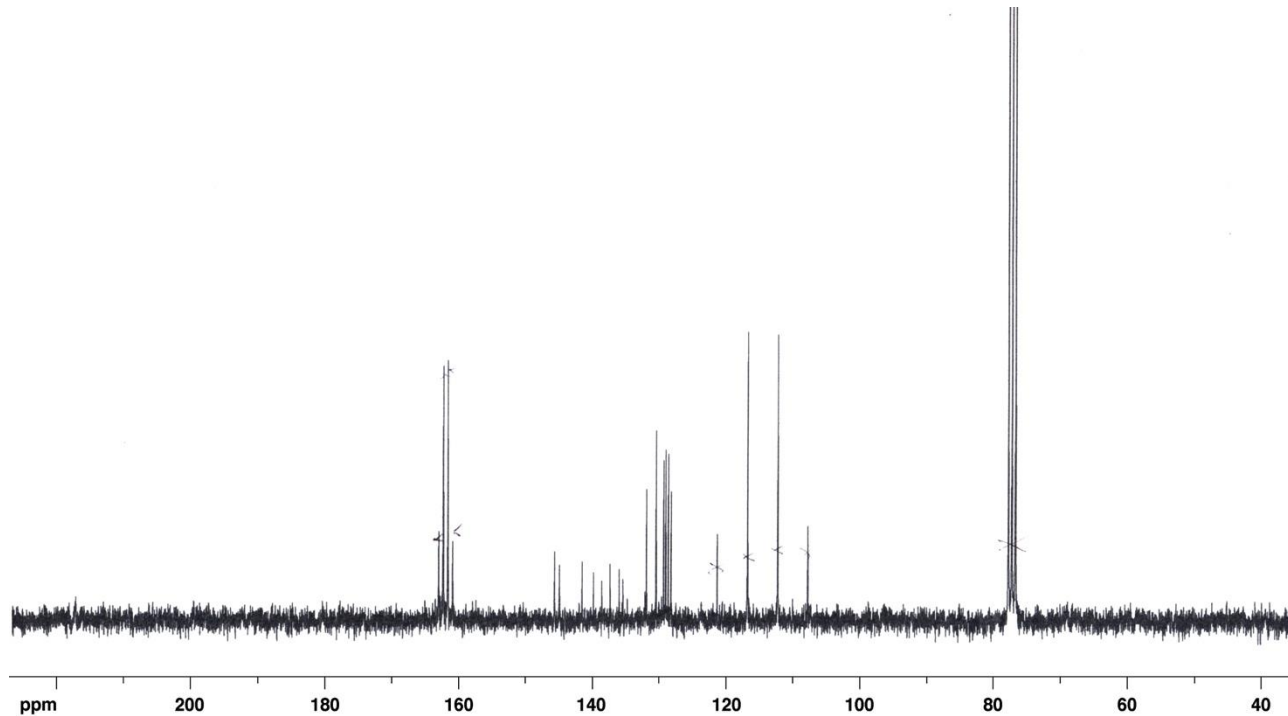


Figure S14: ¹³C NMR spectrum of linear oligomer 7 (62.5 MHz, CDCl₃/CF₃COOH 5/1 v/v). Note: the strong quartet resonances centred at 114 and 162 ppm are due to trifluoroacetic acid co-solvent.

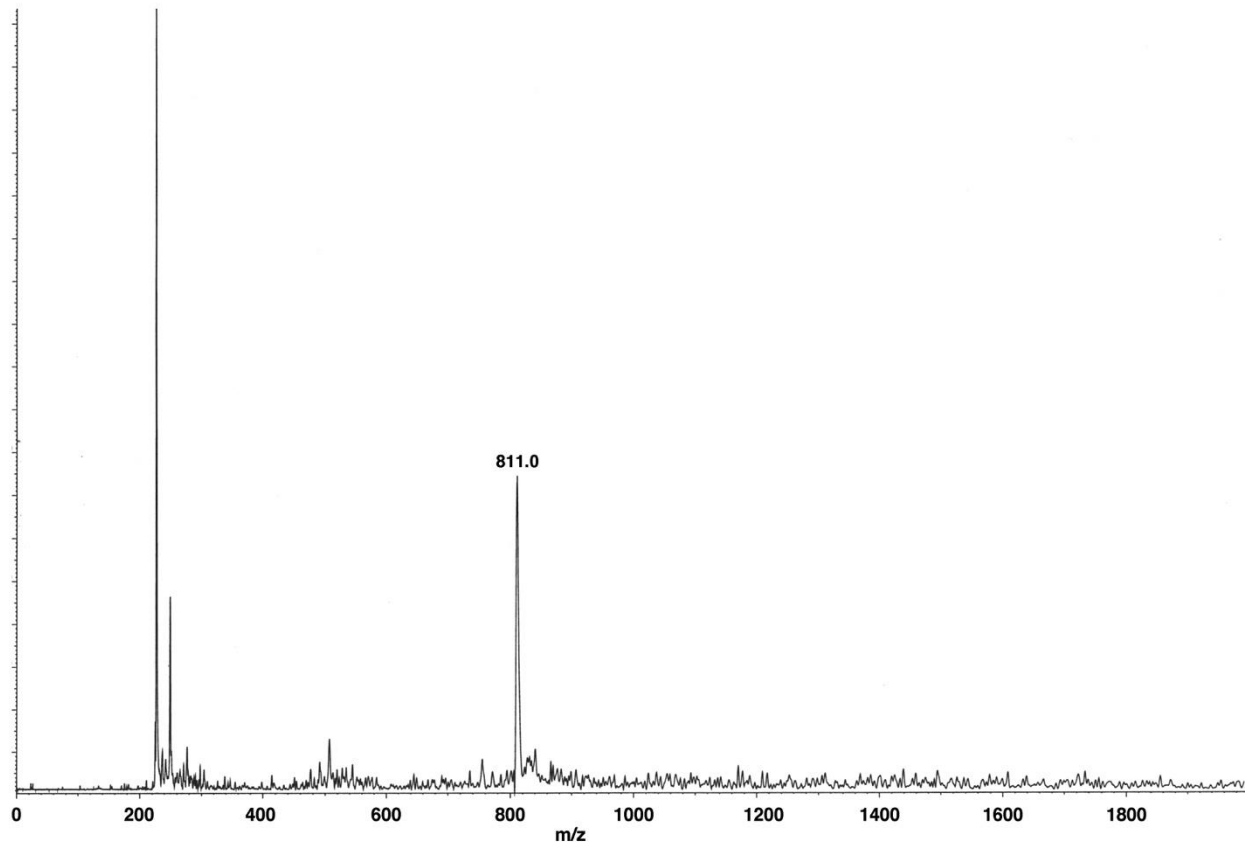


Figure S15: MALDI-TOF mass spectrum of linear oligomer **7**. (Calc. m/z for $[C_{44}H_{28}S_2O_6Cl_2Na]^+ = 810.7$).

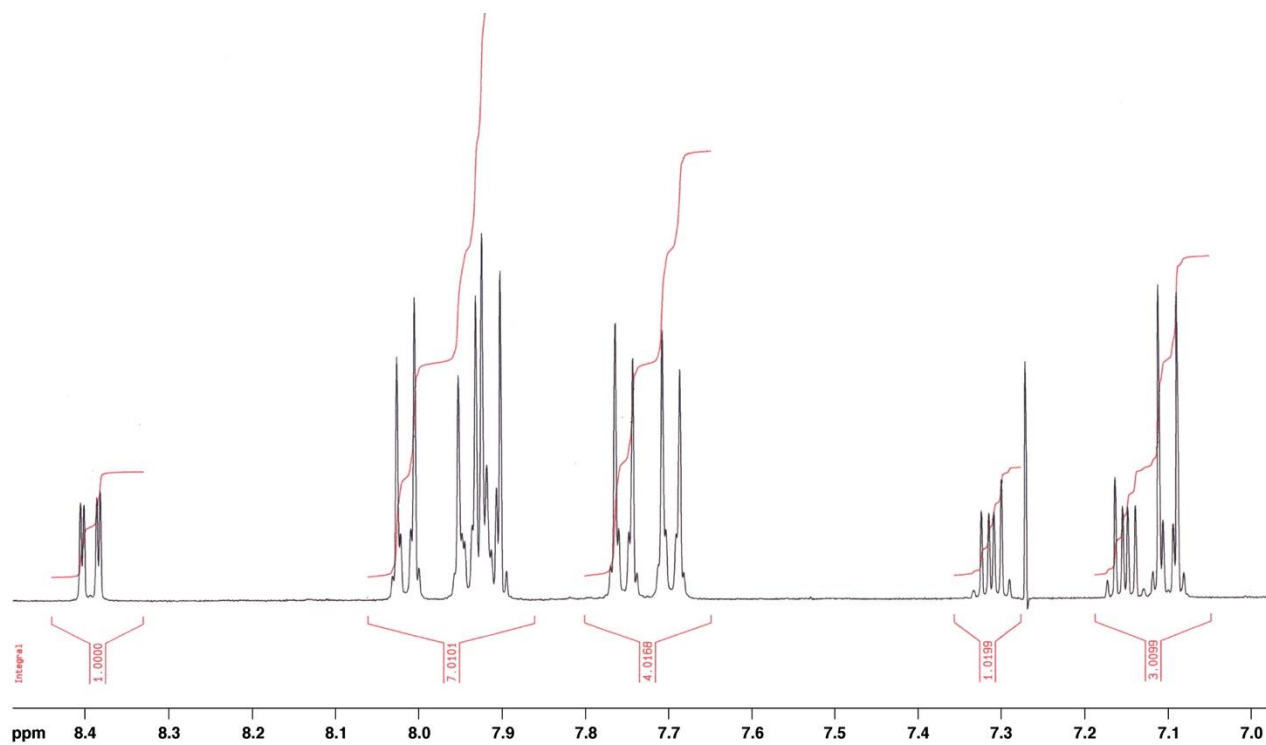


Figure S16: ¹H NMR spectrum of macrocycle 8 (400 MHz, CDCl₃/CF₃COOH 5/1 v/v).

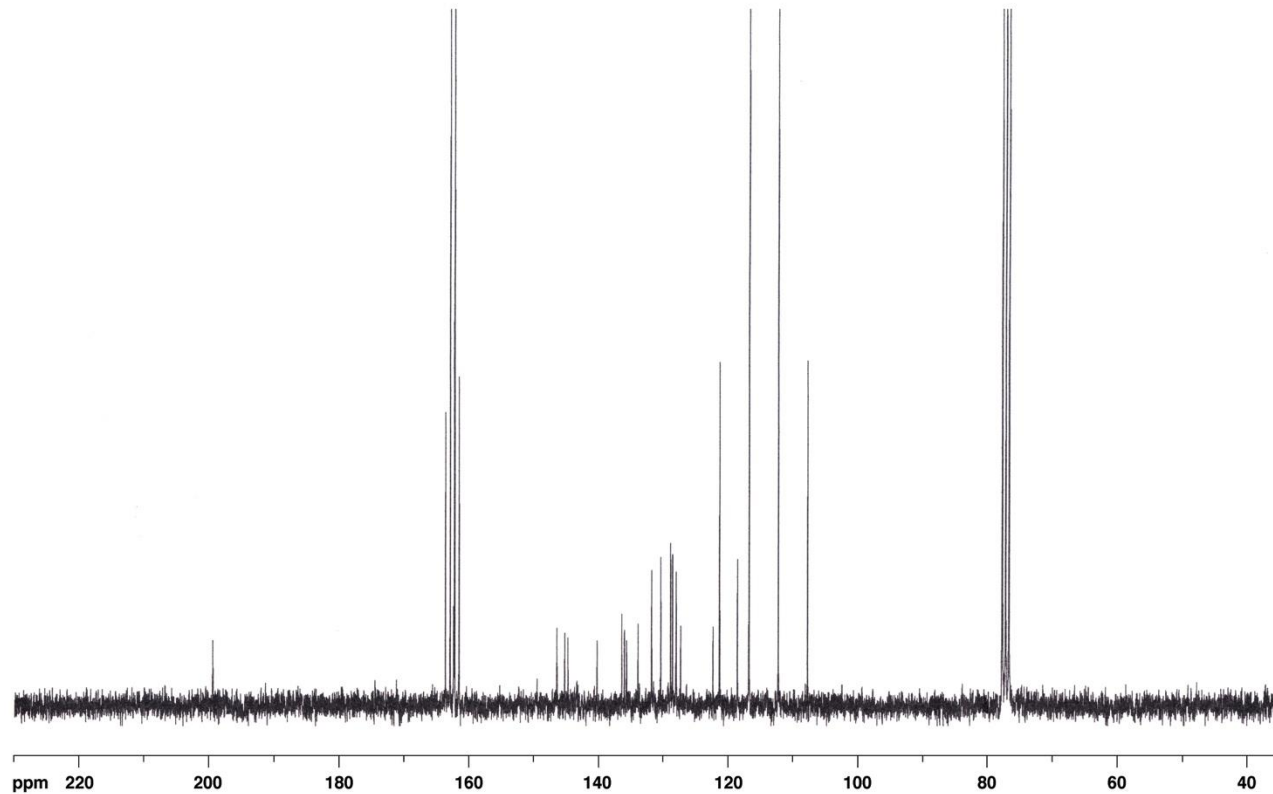


Figure S17: ¹³C NMR spectrum of macrocycle 8 (100 MHz, CDCl₃/CF₃COOH 5/1 v/v). Note: the strong quartet resonances centred at 114 and 162 ppm are due to trifluoroacetic acid co-solvent.

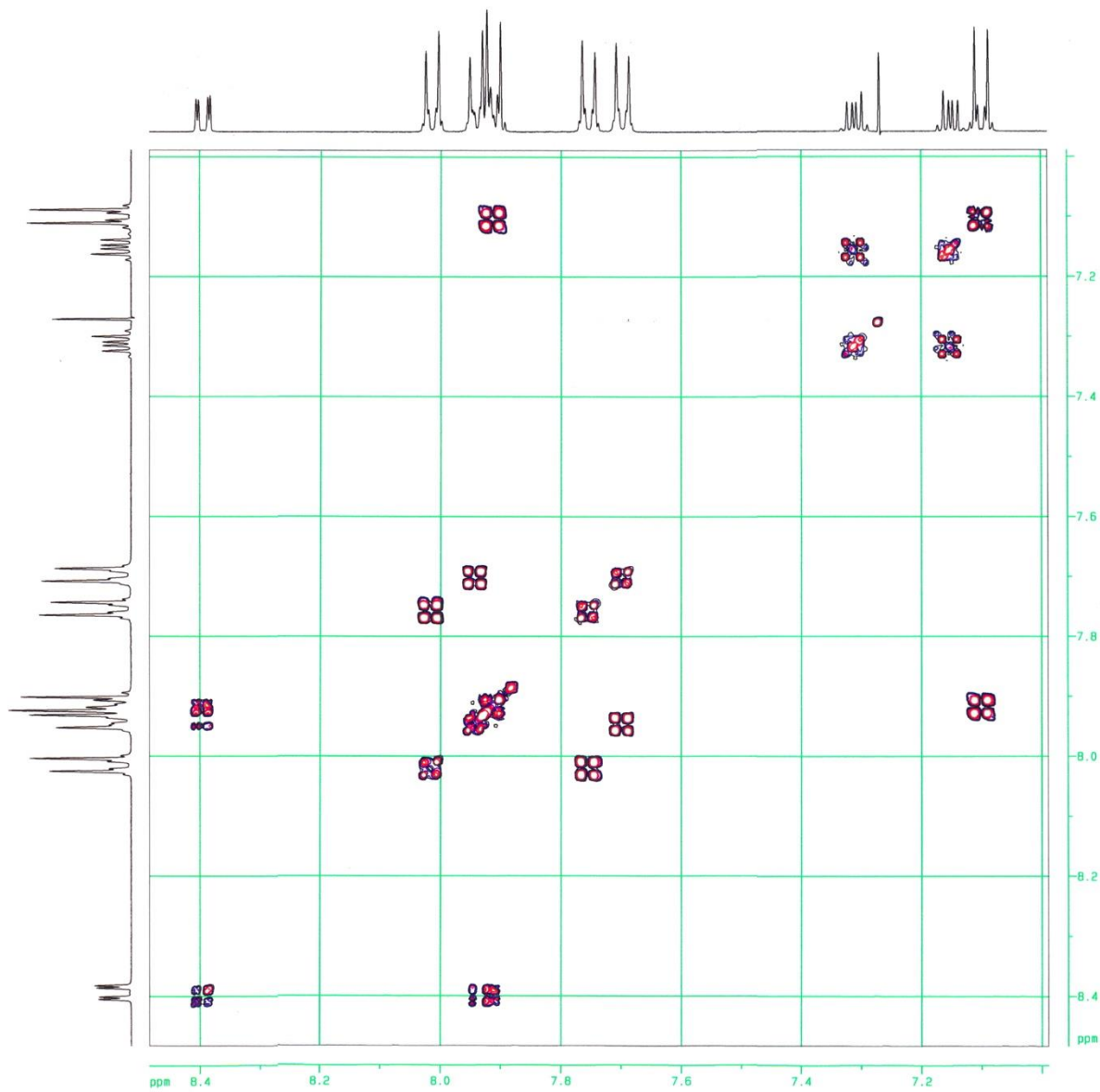


Figure S18: ^1H - ^1H COSY NMR spectrum of macrocycle **8** (400 MHz, $\text{CDCl}_3/\text{CF}_3\text{COOH}$ 5/1 v/v).

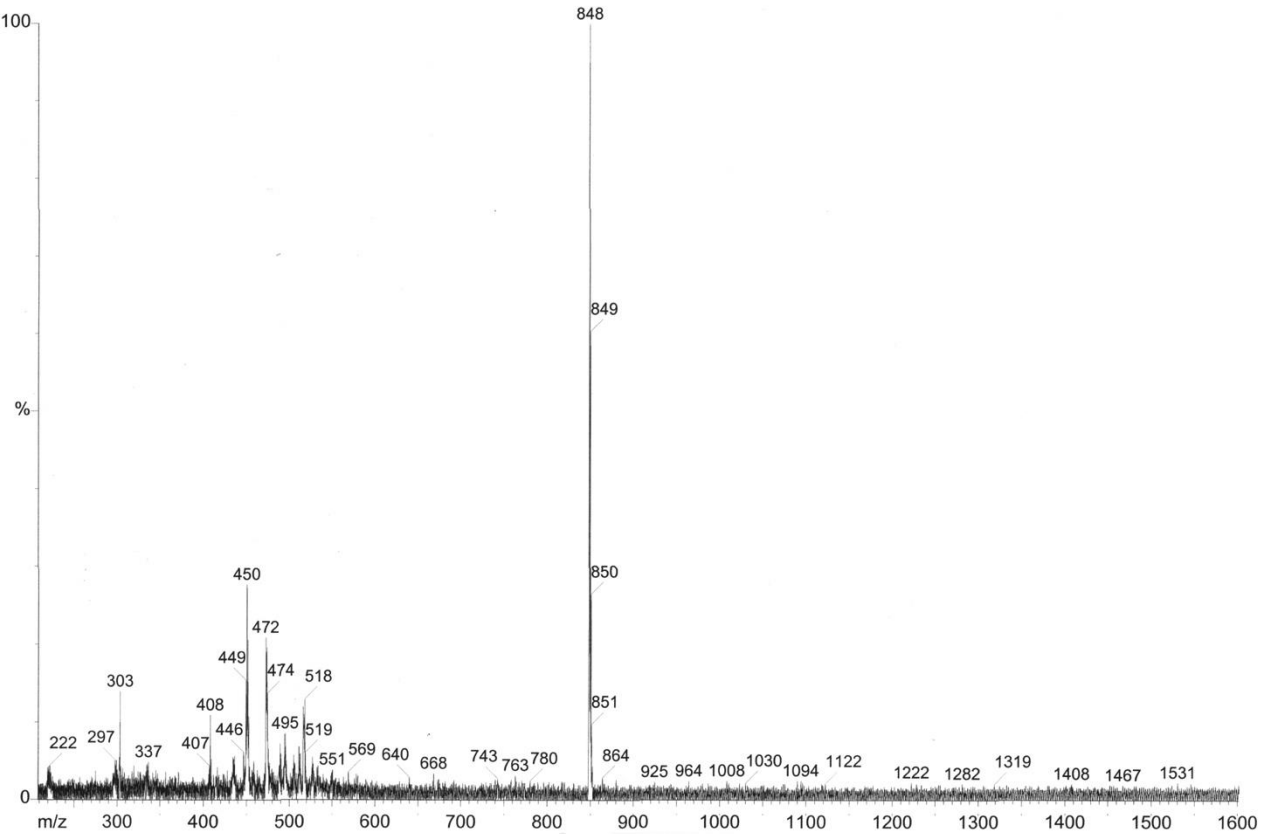


Figure S19: MALDI-TOF mass spectrum of macrocycle **8** (Calc. m/z for $[C_{50}H_{32}S_2O_8Na]^+ = 847.9$).

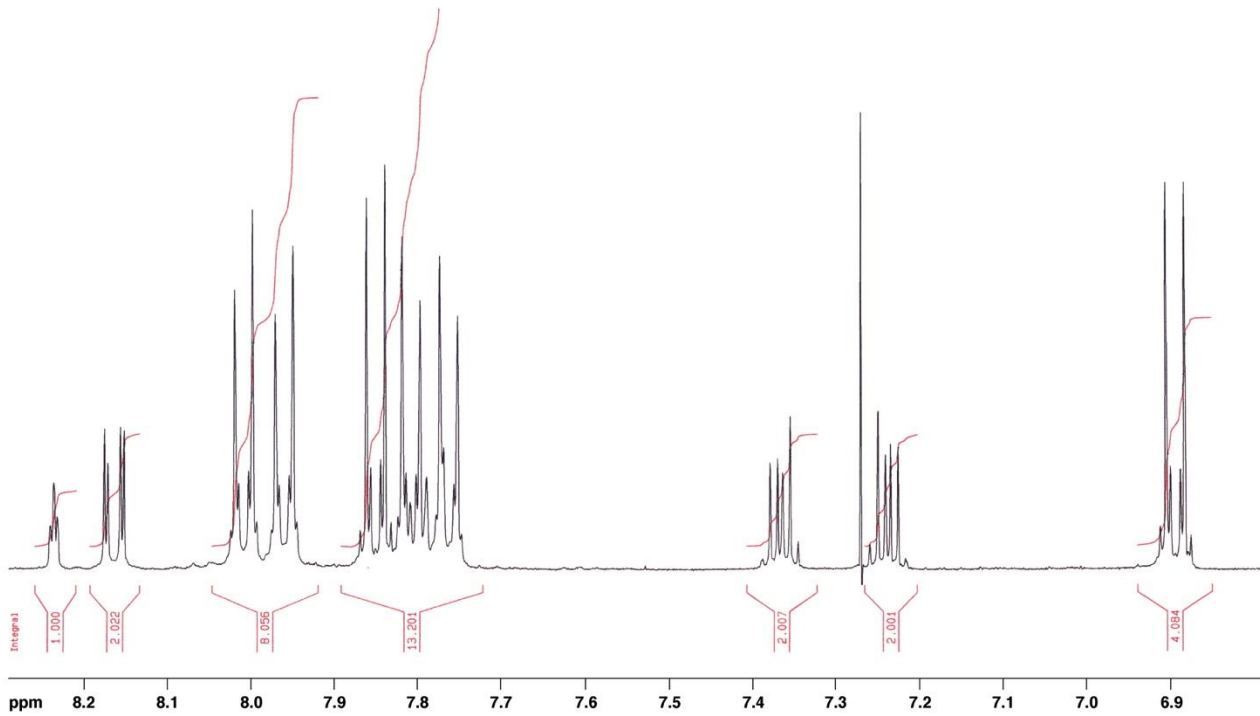


Figure S20: ¹H NMR spectrum of macrocycle 9 (400 MHz, CDCl₃/CF₃COOH 5/1 v/v).

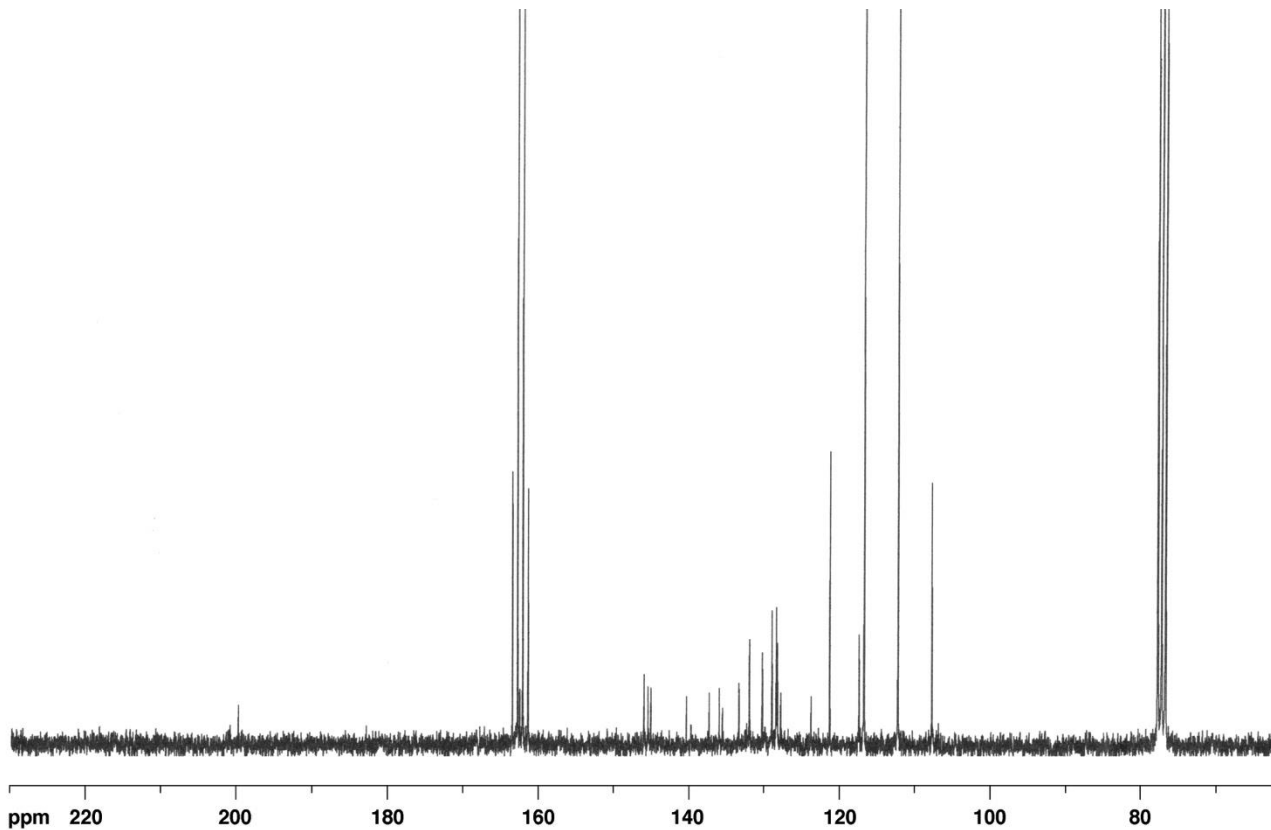


Figure S21: ¹³C NMR spectrum of macrocycle 9 (100 MHz, CDCl₃/CF₃COOH 5/1 v/v). Note: the strong quartet resonances centred at 114 and 162 ppm are due to trifluoroacetic acid co-solvent.

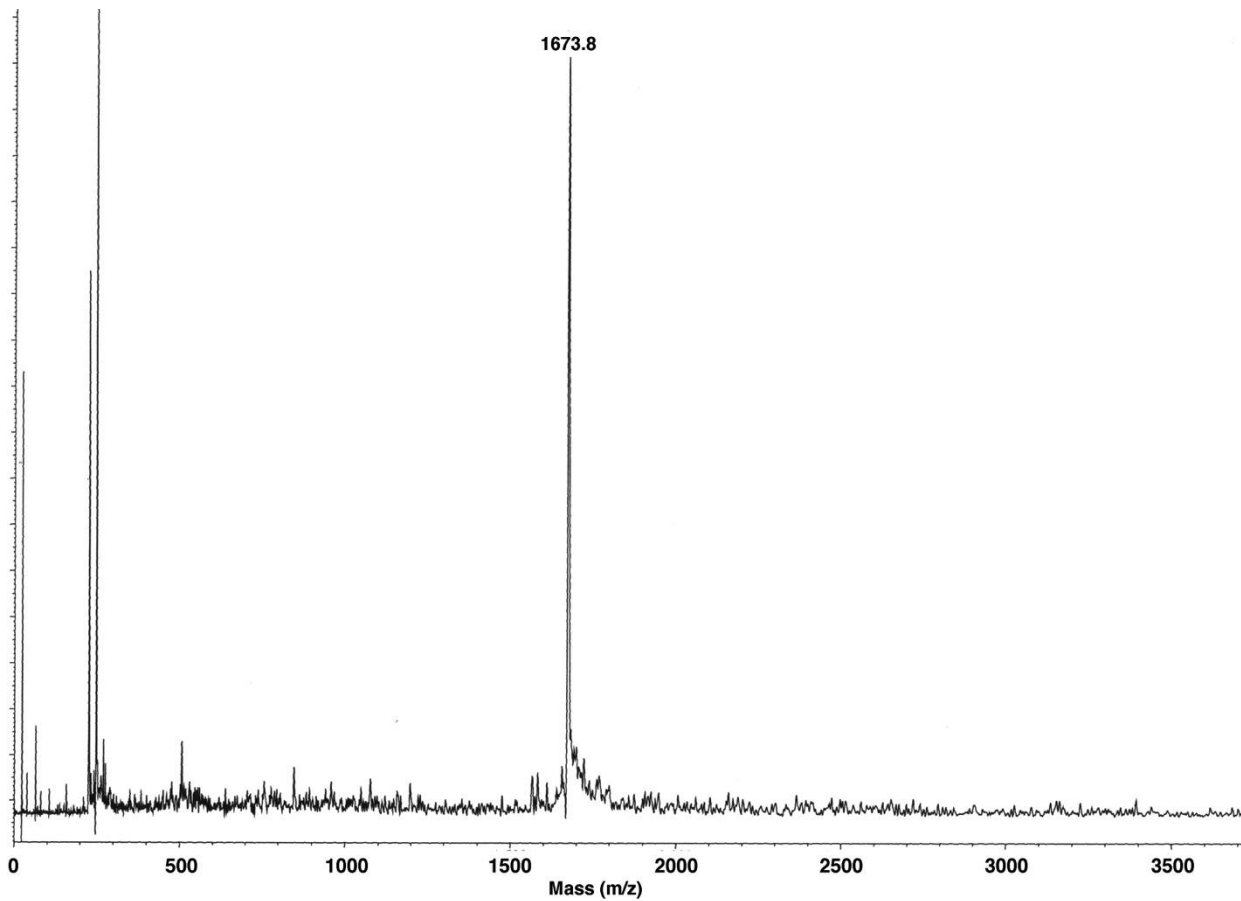


Figure S19: MALDI-TOF mass spectrum of macrocycle **9** (Calc. m/z for $[C_{100}H_{64}S_4O_{16}Na]^+ = 1672.8$).

Computational modelling of macrocycles **8** and **9**

Models of macrocycles **8** and **9** were constructed on a SGI-O2 workstation using the *Cerius2* suite of programs, v. 3.5, Accelrys, San Diego. Models were minimised initially using the Dreiding-II force field (molecular mechanics with charge-equilibration),^{S1} and the resulting models were then re-minimised with a modified version of this force field in which aromatic ether, ketone, and sulfone linkages were constrained to experimentally-established bond lengths and bond angles.

Atomic coordinates of the final models for **8** and **9** are available from the authors as electronic data files in pdb format. Email: fabio.arico@unive.it; or h.m.colquhoun@rdg.ac.uk

S1. Mayo, S. L.; Olafson, B. D.; Goddard III, W. A. *J. Phys. Chem.* **1990**, *94*, 8897-8909.